HHS Public Access

Author manuscript

Neuroimage. Author manuscript; available in PMC 2020 May 27.

Published in final edited form as:

Neuroimage. 2020 February 15; 207: 116390. doi:10.1016/j.neuroimage.2019.116390.

The Relationship between BOLD and Neural Activity Arises from Temporally Sparse Events

Xiaodi Zhang[1], **Wen-Ju Pan**[1], **Shella Dawn Keilholz**[1,*]

[1]The Wallace H. Coulter Department of Biomedical Engineering, Georgia Institute of Technology and Emory University, Health Sciences Research Building, 1760 Haygood Drive, SuiteW200, Atlanta, GA 30322, USA

Abstract

Resting state functional magnetic resonance (rs-fMRI) imaging offers insights into how different brain regions are connected into functional networks. It was recently shown that networks that are almost identical to the ones created from conventional correlation analysis can be obtained from a subset of high-amplitude data, suggesting that the functional networks may be driven by instantaneous co-activations of multiple brain regions rather than ongoing oscillatory processes. The rs-fMRI studies, however, rely on the blood oxygen level dependent (BOLD) signal, which is only indirectly sensitive to neural activity through neurovascular coupling. To provide more direct evidence that the neuronal co-activation events produce the time-varying network patterns seen in rs-fMRI studies, we examined the simultaneous rs-fMRI and local field potential (LFP) recordings in rats performed in our lab over the past several years. We developed complementary analysis methods that focus on either the temporal or spatial domain, and found evidence that the interaction between LFP and BOLD may be driven by instantaneous co-activation events as well. BOLD maps triggered on high-amplitude LFP events resemble co-activation patterns created from rs-fMRI data alone, though the co-activation time points are defined differently in the two cases. Moreover, only LFP events that fall into the highest or lowest thirds of the amplitude distribution result in a BOLD signal that can be distinguished from noise. These findings provide evidence of an electrophysiological basis for the time-varying co-activation patterns observed in previous studies.

Keywords

resting state fMRI; BOLD; electrophysiology; instantaneous co-activation; BOLD-triggered average

1. Introduction

Functional magnetic resonance imaging (fMRI) is a noninvasive method that uses the blood oxygenation level- dependent (BOLD) (Ogawa et al., 1992) signal to measure the neural activity in different parts of the brain. In resting state fMRI (rs-fMRI) (Biswal et al., 1995), a statistical relationship between the spontaneous activity of different areas of the brain in the

*Corresponding author. shella.keilholz@bme.gatech.edu (Shella Keilholz).

absence of an explicit stimulation or task indicates that the regions are functionally related (Biswal et al., 1995; Fox and Raichle, 2007). Temporal correlation is often used to measure this functional connectivity, and the spatial patterns of the BOLD signal correlation show high similarity to many established brain networks, including motor, visual, language, default mode, and attention networks (Biswal et al., 1995; Cordes et al., 2000; Hampson et al., 2002; Greicius et al., 2003; Fox et al., 2006; Smith et al., 2009). However, as an imaging method, rs-fMRI inevitably suffers from physical limitations on its temporal resolution (~1s), as well as the fact that neural activity is measured indirectly though neurovascular coupling (Logothetis et al., 2001).Recent rs-fMRI studies, using paradigm free mapping (PFM) (Gaudes et al., 2011; Gaudes et al., 2013; Petridou et al., 2013), point process analysis (PPA) (Tagliazucchi et al., 2011, 2012a), or co-activation patterns (CAPs) (Liu and Duyn, 2013, Liu et al., 2013) have shown that the BOLD information is compressed into a few temporally sparse events. It was shown that averaging these sparse activation events yields resting state network (RSN) patterns that are very similar to the conventional seed-based correlation map, which requires the utilization of the entire dataset. Moreover, the CAPs approach also has shown that those activation events can be further divided into several subgroups that show specific spatial patterns, suggesting that there might be some dynamic organization of the brain. Following their findings, there are several CAP studies performed on human (Wu et al., 2013; Amico et al., 2014; Li et al., 2014; Allan et al., 2015; Chen et al., 2015; Tagliazucchi et al., 2016; Liu et al., 2018a; Turchi et al., 2019), rodents (Liang et al., 2015) and monkeys (Liu et al., 2018).

While these approaches that focus on discrete BOLD events instead of a continuous interaction between brain regions have provided new insights into brain function, they usually rely on the BOLD signal, which is an indirect measurement of neural activity. To better understand the neuronal origin of the CAPs observed in fMRI studies, another modality that more directly measures neuronal activities is needed (for review, see Keilholz, 2014). Logothetis et al. (2001) pioneered the development of simultaneous acquisition of local field potentials (LFP) and fMRI data in primates. Since their initial work, there are increasing number of studies that have simultaneous LFP and fMRI data acquisition (Shmuel et al., 2006; Huttunen et al., 2008; Shmuel et al., 2008; Murayama et al., 2010; Pan et al., 2011; Mishra et al., 2011; Magri et al., 2012; Devonshire et al., 2012; Pan et al., 2013, Garth et al., 2014). However they typically draw a region of interest (ROI) to study the relationship between LFP and BOLD, and the potential useful information in the other regions of the brain is discarded. Also, the recent approaches in BOLD-fMRI that focus on high amplitude events provide many meaningful insights into dynamic resting state networks. Therefore, using methods similar to CAPs in multimodal neuroimaging may give supplementary information that cannot be discovered using conventional correlation analysis alone.

But to our best knowledge, there are only a few studies that use multimodal neuroimaging methods to study the neuronal origin of the dynamic resting state networks. Tagliazucchi et al. (2012b) performed simultaneous EEG and fMRI recording in human, and found a very interesting result: the fluctuation in BOLD signal functional connectivity is positively correlated with the local synchronization of EEG gamma band power. Another very intriguing phenomenon was revealed in the simultaneous LFP and fMRI recordings in

monkey performed by Liu et al. (2018a). They demonstrated that the fMRI global signal peaks co- occur with sequential spectral transitions (SST) in LFP, which is a spectral shift toward low frequencies.

In this paper, we investigate two key questions about the neural basis of rs-fMRI: 1) Do the BOLD events that are the basis of co-activation patterns reflect distinct, high amplitude neural events? 2) Is there a range of neural activity which reliably produces a BOLD response that can be distinguished from noise? Inspired by the idea of the spike-triggered average (Dayan and Abbott, 2001) and co-activation patterns (CAPs) (Liu and Duyn, 2013), we propose two new methods called the BOLD-triggered average of LFP power (referred to as the BOLD-triggered average in the rest of the article) and LFP-triggered co-activation patterns (LFP-CAPs) to see if the relationship between LFP and BOLD is driven by discrete high-amplitude events. The BOLD-triggered average shows the average time course of LFP power preceding high amplitude BOLD events, whereas the LFP-CAPs average the fMRI frames a certain lag (depending on the anesthetic agents) after high amplitude broadband LFP events to show the spatial distribution of the brain regions that “co-activate” with the neuronal activity recorded by LFP. The two methods provide complementary information in both the temporal and spatial domains, and the results suggest that the relationship between LFP and BOLD is also driven by a few distinct events that have the highest amplitudes in either the BOLD or LFP power. Further analysis shows that those high LFP events can be classified into several groups, producing spatial patterns that are similar to those obtained from the original CAPs method, which solely uses rs-fMRI data.

2. Results

2.1. BOLD-triggered Average of LFP Power Time Courses

The spike-triggered average is widely used for the analysis of electrophysiological data. Each action potential produced by the neuron is considered as an event, which triggers the extractions of the stimulus in a short time window preceding the action potential event. Though the stimuli in the individual windows appear random, the averaged stimulus across all action potential events typically exhibits a pattern that is likely to cause the firing of the neuron, and thus correspond to the receptive field of the neuron. We hypothesize that, if we separate the BOLD time points (BOLD events) into several groups based on their amplitudes, and within each group, average the LFP power time course preceding the BOLD events, we may get a pattern in LFP power (both in temporal domain and frequency domain) that is likely to cause the occurrence of a BOLD event with a specified amplitude.

To test our hypothesis, we analyzed 337 simultaneous single slice fMRI and primary somatosensory cortex (S1) LFP recordings from both hemispheres from 36 Sprague–Dawley rats (male, 200–300 g, Charles River) under isoflurane (ISO. n = 100) ranging from 1% to 2%, or dexmedetomidine (DMED, n = 237) anesthesia on a 9.4T/20 cm horizontal bore small animal MRI system (Bruker, Billerica, MA). The details of animal preparation and parameter settings for data acquisition are described in section 5. Materials and Methods. For this comparison study, we performed a rigorous data selection procedure using several metrics to ensure that both BOLD and LFP data were of the highest quality. For the LFP data, there were two metrics: the number of gradient artifacts identified, and the noise level

in the LFP signal after removal of gradient artifacts. For the BOLD data, there were four metrics: the residual motion after motion correction, measured by the trajectory of the center of mass and DVARS (Power et al., 2012), image distortion, and function connectivity in bilateral S1 areas. Since there are 1000 TRs and 20 dummy scans, the number of gradient artifacts identified should equal 1020. Some scans have high noise levels that compromise the gradient artifact identification, in which case the number of detected triggers is not equal to 1020. These scans were excluded to eliminate the possibility of residual gradient noise. The rest of the metrics were manually inspected for all scans, and labeled as “good”, “fair” and “poor” (Table 1). Each scan can only have at most one “fair” metric to be selected. By these criteria, 56 scans under ISO and 66 scans under DMED were selected, meaning 63.8% of the entire dataset is not suitable for further analysis. Among the selected 122 scan sessions, the correlation between LFP and the corresponding S1 area for both hemispheres were manually calculated. If both hemispheres show “good” correlation, such dataset was selected for further analysis. By these criteria, 22 scans under DMED and 32 scans under various ISO concentrations were selected out of the 122 scan sessions. This however does not necessarily mean that the rest of the 122 scan sessions are of poor quality. Only 14 scan sessions show “bad” correlation, while the others show “fair” correlation on either or both LFP channels. Note too that the total number of scans includes data acquired immediately after the animal was placed in the scanner and before physiological condition stabilized. We routinely acquire data during this period to allow the detection of any technical difficulties, but the animal condition is rarely optimal. The data and code will be available upon request.

The BOLD signal was extracted from the ROI that has the highest correlation between LFP power and BOLD, which is found near the tip of the electrode. Then both the BOLD signal and LFP broadband power were z-scored and pooled together for by anesthesia (ISO and DMED). Within each dataset, the BOLD signal time points were evenly divided into 10 percentile groups based on their amplitudes. Figure 1 illustrates the process of obtaining the BOLD-triggered average time course. First the percentiles were calculated from the pooled distribution to obtain the thresholds for each percentile group (shown in the color-coded histogram), and the time points within the thresholds were selected as the triggers. Then the LFP broadband power time course preceding each BOLD trigger was extracted and averaged across all fMRI scans, and the resulting time course is referred to as the “BOLD-triggered average”. Please note that, although as a physical value LFP power is non-negative, it can become negative after normalization, because both band-pass filtering and taking the z-score remove the direct current (DC) component. The adjacent triggers are considered as separated triggers, though alternatively one could make them become a single trigger, weighted by the duration of the event. The two methods produce very similar results (see Supplemental Materials, Figure S.1); we used the former for the rest of the paper.

Note that the process can be applied to the LFP power in other frequency bands as well, and the BOLD-triggered averages obtained in different frequency bands are directly comparable with each other, because they all share the same BOLD triggers and are therefore aligned along the time axis. Figure 2 shows the BOLD-triggered average of LFP power in six frequency bands (delta 1~4Hz, theta 4~8Hz, alpha 8~12Hz, low frequency beta 12~25Hz, high frequency beta 25~40Hz and gamma 40~100Hz) as well as the broadband power, which is the sum across the six frequency bands.

Generally speaking, the BOLD-triggered average shows that the LFP-BOLD relationship is monotonic. Before the strong positive BOLD events (70~100 percentiles), the LFP power exhibits an increased amplitude, whereas before the strong negative BOLD events (0~40 percentiles), the LFP power exhibits a decreased amplitude. The peak change occurs at a time lag in line with previous findings (Pan et al., 2013), which is 4 seconds under ISO and 2.5 seconds under DMED. For the BOLD events with an amplitude around the median value (40~70 percentiles), the LFP power shows a consistent trend (LFP power increases before a BOLD event higher than median value, and decreases before a BOLD event lower than median value), however, the effect is not significant enough to be distinguished from the general noise of the time courses. The 95% confidence interval of the random fluctuations is estimated by manually labeling the segments of BOLD-triggered average with a lag of −30 ~ −15 seconds and 5 ~ 20 seconds as the “noise” or irrelevant time segments, which provides 600 time points for the empirical estimation of the noise distribution. The aforementioned LFP power percentiles that significantly differ from the noise (70 ~ 100% for positive BOLD events and 0 ~ 40% for negative BOLD events) show some minor variations in the exact percentile values, depending on the anesthetic agents and LFP frequency bands.

Aside from the general trend, there are some additional patterns observed in DMED that are worth noting. First, as the frequency increases from low frequency beta band to gamma band, the time course become heavily contaminated by noise, and most of the percentile levels are no longer significantly different from the noise. This is potentially caused by the low signal-to-noise ratio (SNR) in these high frequency bands under DMED anesthesia, because the energy distribution of LFP decays much faster as frequency goes up when compared to ISO anesthesia (see Figure S.2). Secondly, there is a bipolar structure in delta and theta bands, which means that on average, in addition to the main peak at 2.5 seconds before the event, there is a secondary peak with inversed polarity at 5 seconds before the event, suggesting an anti- correlation between LFP power and BOLD at the time-lag of −5 seconds in these two bands. Since most of the energy is distributed in delta and theta bands, the broadband time course looks like a blend of these two bands.

Figure 3 shows the scatter plot of LFP power and BOLD at the maximally-correlated lag (−4 seconds and −2.5 seconds under ISO and DMED respectively), which provides a general idea about how LFP power is distributed in each BOLD level. It can be seen that while the average value within each cluster (white line plot) shows a clear correlation with BOLD amplitude, individual points have a very widespread distribution. Even for the highest 10% BOLD events, there are still a large number of LFP power occurrences that are below zero. So the increase of LFP power before a high BOLD event shown in Figure 3 is only an average effect, meaning that a high BOLD event does not guarantee an increase in the LFP power. The detailed distributions are provided in Figure S.3. The BOLD-triggered average of the LFP without band-pass filtering is also included in Figure S.4 for comparison.

2.2. LFP Co-activation Patterns

The BOLD-triggered average of LFP power time courses shows that only a portion (0~40% and 70%~100%) of the time courses can be distinguished from the general random fluctuations of the BOLD-triggered averages, which suggests that only LFP power higher

than a certain threshold will trigger a BOLD response (in terms of the averaged effect). This finding is somewhat similar to the findings in co-activation patterns (CAPs) where it is revealed that the interregional BOLD correlations result from instantaneous co-activations of multiple brain regions at some critical time points rather than from continuous, sustained interregional neuronal interactions. We hypothesized that these two findings are tied together and the correlation between BOLD and LFP may be driven by instantaneous co-activations or co- deactivations as well, which might be the physiological reason why the interregional BOLD correlations are driven by instantaneous events.

To test the hypothesis, we proposed a modified version of CAPs that is obtained by applying thresholds to the LFP broadband power time course, as opposite to the original method, which applies thresholds to a selected seed region in the BOLD image series. In this article, the former method is referred to as LFP-CAPs and the latter one is referred to as BOLD-CAPs. To calculate LFP-CAPs, first several thresholds were calculated from the percentiles of LFP broadband power. For any given threshold, whenever LFP broadband power surpasses the threshold, the corresponding BOLD time frame (4 seconds under ISO, 2.5 seconds under DMED) succeeding the event was extracted. Each voxel was then averaged over the selected BOLD time frames, and the final averaged map was compared with the cross-correlation map between LFP broadband power and BOLD image series using the entire time course. In additional to LFP-CAPs, the original BOLD-CAPs were also calculated for comparison.

Figure 4 shows that as more and more frames are included by lowering the threshold, the spatial similarity between CAPs and the correlation maps increases rapidly, and reaches a plateau above 0.967 after including 10% of the data, suggesting the highest 10% LFP events or BOLD events can accurately replicate the spatial structure in correlation maps. Even a single frame is able to provide a general shape of the correlation map, which implies that the high amplitude events (either high LFP or high BOLD) are dominating the functional networks. These results are generally in line with Liu et al. 2013.

In addition, the highest 15% BOLD time frames were selected for temporal decomposition (the BOLD-CAPs only need 5% to resemble the spatial pattern, but to avoid randomness caused by extremely small sample size, the threshold was set to 15%). K- means clustering was performed on the selected BOLD time frames (the distance was defined as 1 minus Pearson correlation coefficient), and the within cluster averages produce the temporal decomposition of the co-activation patterns. Liu and Duyn (2013) selected the number of clusters k as 8 for posterior cingulate cortex region, and 12 for intraparietal sulcus (IPS) region in human. Liang et al. (2015) calculated the averaged silhouette value to evaluate the quality of clustering. They found 2 clusters had the highest silhouette value, although in the end they chose 3 clusters because it offers the third CAP that shows infralimbic cortex (IL) and hippocampus (HP) connections. As Liu et al. (2018b) mentioned, the target number of CAPs to be classified is hard to determine. Since the single slice EPI scans in rodents contains less information than the whole brain EPI scans in human, we chose to use fewer clusters. The 6 clusters we obtained in this study all show distinct spatial patterns and have comparable occurrence rates. So none of them appear to be trivial, and the 3 clusters used by Liang et al. (2015) may be too few to catch all of the information contained in our LFP-

BOLD dataset. We also calculated the K means clustering results with K=3, K=8 and K=10 (see supplemental materials, Figure S.8), which demonstrated that K=8 and K=10 both show some redundant CAP patterns. Therefore K=6 is around optimum for this particular dataset.

It can be observed both visually from the patterns themselves and the similarity matrix that, despite some differences, most LFP-CAPs and BOLD-CAPs are highly spatially similar to each other (see Figure 5). The 2 by 2 quasi-diagonal elements in bright yellow can be easily distinguished from the other elements, suggesting that the intra-CAPs similarities are high among LFP- CAPs and BOLD-CAPs, and the inter-CAPs similarities vary. It is worth noting that the similarity between LFP-CAPs and BOLD- CAPs is not the result of overlapping triggers, because the high LFP events and high BOLD events only have 25.6% overlap in the time domain (see Figure S.5). Other factors (like network structure) that affect network dynamics may account for the similarity. There is also an intra-CAPs similarity observed across ISO and DMED (marked by the red dotted line), which can be distinguished from other inter-CAPs similarities, but the correlation values are not as high as the ones within the same anesthetic agents. This suggests when the anesthesia changes from ISO to DMED, the instantaneous functional networks change in some ways, but retains certain properties of spatial organization. It is worth noting that the correlation maps obtained from the conventional correlation analysis are visually very similar in these two cases despite the distinct mechanisms of anesthesia under the two agents. This suggests that the CAPs method is more sensitive to anesthetic-related changes than the conventional correlation analysis, possibly because it better preserves information about network dynamics.

3. Discussion

3.1. General Findings

In this study, we utilized two complementary methods for the analysis of simultaneous rs-fMRI and LFP recording data to show that the correlation between BOLD and LFP is mainly influenced by discrete high amplitude events. The high amplitude LFP power events not only show an increased likelihood of eliciting a localized BOLD response, but also produce co-activation patterns that are nearly identical to the cross correlation map between LFP and BOLD. Furthermore, the co-activation events can be clustered into several distinct groups. While it is not surprising that high amplitude LFP events result in co-activation patterns similar to those obtained from BOLD alone, since high amplitude BOLD events drive correlation between areas, and BOLD is linked to LFPs. However it is also entirely possible a different network patterns triggered by LFP events. So the results presented here provide electrophysiological evidence of neural underpinnings for the multiple BOLD-CAPs obtained from rs-fMRI data.

3.2. On average, the LFP power preceding the BOLD events exhibits a stereotypical profile.

BOLD-triggered averaging revealed that there are certain temporal patterns that manifest before a BOLD event. The increase or decrease of LFP power from baseline peaks at 4 seconds before the BOLD response under ISO, and 2.5 seconds under DMED. This finding is in agreement with the previous studies using conventional cross correlation, but provides

more information about the behaviors of subsets of BOLD time points that have different amplitudes. On average, the high amplitude positive BOLD events (70~100 percentiles) are preferentially preceded by an increase in LFP power, and the negative BOLD events (0~40 percentiles) prefer a decrease in LFP power. This amplitude preference vanishes when the amplitude of BOLD falls into the range near median value (40~70 percentiles), because the changes in LFP power are no longer distinguishable from the random fluctuations. The fact that about 30% of BOLD time points near the median value have no consistent correspondence with the LFP power implies an intrinsic limitation in extracting function connectivity patterns using cross correlation, because a great amount of data that contains little information about neural activity is influencing the result.

Note too that decreases in LFP power precede decreases in the BOLD signal. The origin of the negative BOLD signal has long been debated, given its complicated dependence on neural and vascular parameters. Here we show that during spontaneous activity, decreases in LFP power are closely linked to decreases in the BOLD signal. While this does not rule out other contributions to the negative BOLD effect seen in fMRI (e.g., vascular steal), it does provide support for a neural basis as well.

3.3. The correlation between LFP and BOLD is driven by a few distinct events

The results of LFP-CAPs suggest that, selecting the fMRI frames with the highest 15% of LFP amplitudes can accurately reproduce the spatial patterns seen in the cross correlation map, which requires utilizing the full dataset. This together with the thresholds found in BOLD-triggered average analyses suggest that the relationship between LFP and BOLD is dominated by a few distinct events, specifically those with LFP power amplitude higher or lower than a certain threshold. This finding in a way matches with the previous studies performed by Liu and Duyn(2013) and Tagliazucchi et al.(2012), where it is revealed that the interregional correlation in fMRI are driven by instantaneous BOLD events. Our work confirms that the same principle holds for LFP power recorded at a particular location and the BOLD signal, such that the relationship between the two is driven by a few high amplitude events.

The scatter plots of BOLD vs LFP power make it clear that despite the average relationship between high amplitude LFP events and high amplitude BOLD events, the relationship is highly variable and strong BOLD events can actually be tied to decreases in LFP power. If it were possible to identify the points where BOLD was linked to LFP power (e.g., by incorporating additional information into the analysis), the interpretation of the BOLD signal could be made easier. Unfortunately, our preliminary analysis that considered the length of the LFP burst along with its amplitude did not improve our ability to determine which strong BOLD responses reflected high amplitude LFP events. It may be the case that the noisy relationship between the two signals is fundamental to the processes that mediate neurovascular coupling.

3.4. Frequency Dependence of the BOLD-LFP Relationship and Other Findings

It was reported previously that the BOLD signal preferentially correlates with specific frequency bands of the LFP. The frequency ranges reported were gamma band under ISO

and fentanyl (Logothetis et al., 2001; Shmuel et al., 2008), gamma band under fentanyl and thiopental (Murayama et al., 2010), alpha to gamma band under remifentanil (Magri et al., 2012), delta to gamma band under ISO (Pan et al., 2011, Pan et al., 2013), and delta and theta band under DMED (Pan et al., 2013). The BOLD- triggered average presented in this study is consistent with a frequency preference that is dependent on the anesthetic agent. There is no significant difference among different frequency ranges under ISO, while under DMED, the BOLD-triggered average appears noisier as the frequency increases, especially in the gamma band. These findings are in agreement with the correlation and coherence analysis reported in Pan et al. (Pan et al., 2013), partly because the two studies share similar data preprocessing pipeline and some common datasets. However, other researchers conclude that oftentimes gamma band is the most informative band (Logothetis et al., 2001; Shmuel et al., 2008; Murayama et al., 2010; Magri et al., 2012). The differences might be the result of a shift in the LFP power distribution towards lower frequencies under anesthetics like DMED, which results in very little power at the higher frequencies. This suggests that broadband power, rather than power in any particular band, may prove more a robust predictor of the BOLD signal across anesthetic protocols.

Aside from this, we also found an unexpected phenomenon, which is the bipolar structure in delta and theta bands under DMED. The secondary negative lobe peaks at −5 seconds, which suggests a strong anti-correlation exists between LFP and BOLD. However, this can be only interpreted as an averaged effect obtained from retrospectively regrouping the BOLD time points and may not be essential to trigger the BOLD events. We suspect it arises from the enhancement of delta and theta activity under DMED, creating ongoing oscillations in these frequencies.

Furthermore, a nonlinear relationship between LFP and BOLD is observed under ISO but not DMED. This can be seen from Figure 2 panel A, where the increase of LFP in positive BOLD percentile groups generally has a larger magnitude than the decrease of LFP in negative BOLD groups, and Figure 3 panel A, where the LFP-BOLD line plot clearly shows a curvature. This is a direct evidence that the relationship between LFP and BOLD can be nonlinear and depends on the anesthetic agents. Given the presence of nonlinearity, analysis methods that do not assume linear dependency should be considered instead of Pearson correlation (e.g., mutual information methods presented in Magri et al., 2012).

3.5. Methodological Comparison

There are a few studies that have used similar methodologies. In Liang et al., 2015, CAP studies were performed in awake and anesthetized (1.5% ISO) rats. In their study, whole brain (18 slices) EPI scans with a TR of 1 second were acquired. In our study, we only acquired single slice EPI scan with a TR of 0.5 second, because the gradient-induced artifact in the LFP is too difficult to remove when using multi-slice EPI. They also used averaged silhouette values to determine the optimum number of clusters, which is an interesting thing to study in the future for LFP-CAPs.

A few studies (Tagliazucchi et al., 2012a; Liu et al., 2018; Magri et al., 2012) as well as ours share a common methodology with the spike-triggered average, which has been a well-known method in the field of neuroscience for decades.

In the point process analysis (Tagliazucchi et al., 2012a), it was shown that the averaged BOLD signal around the extracted time points (supra-threshold BOLD events from a seed region) resembles the hemodynamic response function (HRF) evoked by a stimulus. In our study, we averaged the LFP power in different frequency bands, instead of the BOLD signal, but the triggers (supra-threshold BOLD events from a seed region) are the same as the one in the point process analysis.

In the simultaneous LFP and fMRI acquisition Liu et al. (2018) performed on monkeys, the LFP power spectral density function was averaged around the point where the BOLD global signal is higher than a threshold. This approach is actually very similar to ours, except they used the BOLD global signal as the trigger, whereas we used the BOLD signal from a seed region in S1 area as the trigger. The frequency dependency in LFP-BOLD relationship is not entirely in agreement with the findings in Liu et al. 2018. The discrepancy may come from the fact that they used awake monkeys whereas we used rodents under ISO or DMED anesthesia, which show clear anesthesia-dependent effects on the frequency distribution of LFPs.

In Magri et al., 2012, the high gamma LFP power was used as the trigger and the BOLD time courses after the LFP events were averaged. The triggers were then subdivided into three groups based on alpha band or beta band amplitude. While this method is able to show that alpha and beta bands contain complementary information to gamma band, it is difficult to analyze the other frequency bands in any given subgroup, because there are simply too many possible combinations of the subgroups in different frequency bands. On the other hand, in the BOLD- triggered average proposed here, different frequency bands share the same trigger from the BOLD seed region, which simplifies the representation of LFP-BOLD relationship, and makes the different frequency bands directly comparable with each other.

3.6. Implication for Future Studies

Time courses from rs-fMRI are often treated as continuous measurements of the hemodynamic response to neural activity. In reality, most of the information in the time courses appears to be carried by a much smaller set of discrete events, which in turn reflect discrete LFP power events. The finding that only strong LFP events result in a detectable hemodynamic response places fundamental limits on our ability to monitor brain dynamics with hemodynamic-based methods. While low-amplitude ongoing activity in the brain is critical for normal function, only strong excursions from the baseline activity will be detected. This suggests that in rs-fMRI and its relationship to the underlying neural activity, there are a few discrete time points that play more important roles than the remaining time points. Therefore, more emphasis should be put on those critical events, namely those with the highest BOLD amplitudes.

The thresholds for separating events from background fluctuations are dependent on the number of subjects as well as the duration of each scan. By including more data, one can reduce the random fluctuations and thus make the temporal structure of the BOLD-triggered average clearer (similar to SNR). In our analysis, we included 32 scans under ISO and 22 scans under DMED, each lasts 8 min 20 sec. For any single scan without extended acquisition time, the amount of irrelevant data could be more than 30%.

3.7. Technical Limitations

The level of ISO impacts neuronal activity and cerebral perfusion. Mixing datasets with different ISO levels, as done here, could potentially introduce variability in either the BOLD- triggered average time courses or the LFP-CAPs. However, it should be noted that all ISO rats were imaged while in the burst- suppression regime. The number of scans was too small to perform further separation by ISO level. In the future, the impact of varying ISO level on the BOLD-triggered average is worth investigating, and more datasets under different ISO levels are needed.

The datasets used were deliberately chosen to have high LFP- BOLD correlation at the lags corresponding to previously observed hemodynamic delays (−4 seconds under ISO and −2.5 seconds under DMED). While this ensures the overall quality of data, it may introduce some bias as well. In all of our studies, we have found that the correlation coefficient drops drastically in some of the scans even when other scans of the same rat under the same anesthesia with almost identical physiological condition show high correlation. Minor fluctuations in temperature, slow changes in respiration, or other physiological effects of the anesthesia may result in poor data for one scan, which then returns to normal as the physiological parameters are corrected. We monitor rats undergoing simultaneous LFP and MRI very carefully, but it is difficult to keep their condition absolutely stable. The scan sessions that have large head motion, unstable physiological conditions, noisy LFP recordings, or low cross- correlation between LFP and BOLD were discarded. Given the fairly large amount of scan sessions available, we chose the more conservative criteria to ensure the data we selected has the highest quality. In total, we selected 22 scans under DMED and 32 scans under ISO out of 337 scans.

The LFP-CAPs utilize the spatial information obtained from fMRI, taking advantage of the fact the fMRI data are more densely sampled in spatial domain than LFPs, providing additional information about time varying activity that could not be easily discovered using correlation analysis alone. However, this approach is still not ideal, because although LFP is a more direct measurement of the neuronal activity, the LFP appears to be more loosely connected with BOLD signals in other regions, when compared to the BOLD seeded drawn near the electrode (because LFP-CAPs need more frames to reproduce the spatial pattern, as shown in Figure 4). So far we can only confirm that the LFP co- activates with BOLD signals in a similar way that the BOLD seed does, and such similarity can only imply that the apparent time- varying functional connectivity observed in CAPs may be the result of the co-activations of neurons. To collect direct evidence that the resting state networks are dynamic and are driven by discrete events, one needs to use multiple electrodes located in areas throughout the network. Such an experiment has many technical difficulties, and LFP-CAPs remain a good alternative to provide spatial information until the successful implementation of multi-region, high-resolution LFP recording and MRI.

Finally, it appears that the anesthesia agent used can substantially influence the spatial organization of neural activity (represented by BOLD-CAPs and LFP-CAPs in this study), as well as the frequency dependency of the LFP-BOLD relationship. It is not surprising to see that ISO and DMED produce different CAPs and BOLD triggered averages, because the underlying physiological conditions appear to be quite different. Isoflurane is a vasodilator

and dexmedetomidine is a vasoconstrictor. Both change the cerebral blood flow as well as the cerebral blood volume, which ultimately may influence the BOLD signal. Also, high ISO concentration tends to reduce the spatial localization of functional connectivity, whereas DMED induces a neural state very similar to natural sleep without deeply suppressing central nervous system (CNS) activity (Magnuson et al., 2014). The hemodynamic response functions (HRF) have different peak times (4 seconds under ISO and 2.5 seconds under DMED), reflecting changes in the vasculature. The LFP power spectral density function shows more high frequency components under ISO than under DMED. Last but not least, under ISO the neurons tend to rapidly fire in a short period of time, often in a timescale of a few seconds, and then rest for a few seconds before starting rapid firing again. This phenomenon is known as the burst- suppression and is very prominent when the ISO concentration is high (Liu et al., 2010, Pan et al., 2011). So with these apparent differences in ISO and DMED anesthesia conditions, and the discrepancy among our study and the other studies using different anesthetic agents, it can be seen that the anesthetic agent plays a very important role in fMRI studies, as well as other concurrent neurophysiological recording studies. The underlying mechanism of how the dynamic functional connectivity and the frequency dependency of the LFP-BOLD relationship is altered by the anesthetic agent still remain an open question, and it is worthwhile to investigate in the future.

4. Conclusion

To conclude, in this article we proposed two methods to analyze simultaneous fMRI and LFP recording data: the BOLD- triggered average and the LFP-CAPs. The BOLD-triggered average shows that the there is a particular temporal pattern in the LFP power shortly before any type of BOLD events, especially those events with the highest BOLD amplitudes where the pattern of LFP power stimulus is most easily distinguished from the background noise. Under different anesthesia, the temporal patterns in the averaged LFP power show different frequency preferences.

The spatial similarities between the LFP-CAP and the cross correlation map suggests that the relationship between LFP and BOLD is driven by instantaneous co-activations or co-deactivations , which is in line with the finding in BOLD-triggered averages that the averaged LFP stimulus will exhibit some noticeable patterns only if the BOLD triggers are high in amplitude The spatial similarities between LFP-CAPs and BOLD- CAPs suggests that the time-varying resting state networks found in fMRI studies may be attributed to the time-varying behavior of LFP in different brain regions, although the underlying mechanism is still not fully understood.

5. Materials and Methods

5.1. Animal Preparation

All animal experiments were performed in compliance with NIH guidelines and were approved by the Emory University Institutional Animal Care and Use Committee. Previously acquired data from 36 Sprague–Dawley rats (male, 200–300 g, Charles River) were used in this study. A full description of the methods is given in the prior publication (Pan et al., 2011) and summarized here. All rats were anesthetized with 2% isoflurane

during surgery. Fine tip electrodes (~10 μm in diameter, borosilicate pipettes) were prepared with micropipette pullers (PE-2; NARISHIGE). The electrodes were filled with artificial cerebrospinal fluid (ACSF), resulting in an impedance of 1 – 5MΩ between the chloridized silver wire and the extracellular environment. The details of the surgical procedures and microelectrode implantation have been described in (Pan et al., 2010). A pair of micro-glass electrodes was implanted in S1FL of the left and right hemispheres separately and secured to the skull using dental cement (methyl methacrylate) for all rats. In order to reduce the MRI artifacts caused by susceptibility, a layer of toothpaste (Colgate, NY) was applied to replace the removed skin and muscle over the skull, and also the dental cement was used at the area >0.5 mm posterior to the imaging slice.

5.2. Simultaneous fMRI imaging and LFP recording

All imaging was performed on a 9.4T/20 cm horizontal bore small animal MRI system (Bruker, Billerica, MA). A three-plane scout image was first acquired to position the fMRI scans. To improve the homogeneity of the magnetic field, the volume of interest (6 mm^3) was shimmed using FASTMAP (Gruetter 1993). Manual shimming adjustment was then applied when necessary to improve the field homogeneity of the selected slice. For fMRI studies, a coronal imaging slice was selected to cover bilateral S1FL areas, in which the glass recording electrode tips were implanted. The EPI imaging parameters were FOV, 1.92 × 1.92 cm^2; matrix size, 64 × 64; in-plane resolution, 0.3 × 0.3 mm^2; slice thickness, 2 mm; and TR/TE, 500/15 ms. A total of 337 resting state scans were collected under several different concentrations of isoflurane ranging from 1% to 2%. (ISO, n = 100) or dexmedetomidine (DMED, n = 237) anesthesia. The isoflurane, in a mixture of 70% O2 and 30% room air, was continuously delivered to the nosecone, allowing for free breathing throughout the experiment. The rat's oxygen saturation, measured with a pulse oximeter, was kept above 98% throughout the data acquisition process. For DMED studies, a bolus of 0.025 mg/kg dexmedetomidine was injected subcutaneously. Isoflurane was disconnected 10 min afterwards, and switched to a continuous subcutaneous infusion of dexmedetomidine (0.05 mg/kg/h). The dose was increased by a factor of three (0.15 mg/kg/h) after ~1.5 h, following the protocol for prolonged sedation described in (Pawela et al., 2009). The DMED scans were conducted >3 h after switching from ISO to avoid any residual ISO effects (Magnuson et al., 2014). The fMRI image acquisition lasts 8 min 20 sec (1000 TR), and 20 dummy scans were acquired to reduce transient signal intensity fluctuations at the start of the image series, which makes the total length of LFP segments that contains gradient-induced artifacts become 8 min 30 sec. Because the whole dataset was acquired over a period of several years, there were two sets of recording parameters: 1. (×500 amplified, 0–100 Hz band-pass filtered, 60 Hz notch-filtered, 12 kHz sampling rate, and ~10 min acquisition length) and 2. (×1000 amplified, 0.1 Hz–5 kHz band- pass filtered, 60 Hz notch-filtered, and 12 kHz sampling rate, and ~14 min acquisition length). The LFP recording lasts longer than the image acquisition to record the LFP without the gradient- induced artifacts, which provides a benchmark for the artifact- removal algorithm. There are two LFP recording segments before and after the image acquisition that last either around 1 min or around 3 min, depending on the parameter sets. However, these differences in the recording parameters will not compromise the analysis because in the data processing the LFP was all band-pass filtered to 0.1–100Hz, the amplitude was normalized, and the excessive LFP

segments were truncated to match the length of fMRI data. A 16 bit analog-to-digital converter (PCI-6281; National Instruments) was used for analog to digital conversion. All physiological parameters were monitored and maintained within normal ranges, including rectal temperature, respiration rate, SpO2/cardiac rate. The animals were sacrificed at the end of the experiment.

5.3. LFP Data Pre-processing

The electrophysiological signal recorded during fMRI scans contains neural signals and gradient-induced artifacts, which are easily distinguished by their high amplitudes. These gradient- induced artifacts were removed offline in MATLAB (Mathworks) following a similar procedure to that illustrated in (Pan et al., 2011). To identify the time when gradient-induced artifacts are present, the rising edge is captured by comparing the first order derivative with a predefined threshold. If the total number of the detected gradient-induced artifacts equals to 1020 (the duration of fMRI scan was 1000 TRs, and there were 20 dummy scans before the actual data acquisition), the LFP data was then proceeded to the next step. Otherwise if the artifacts are not identified correctly due to the presence of some large noise spikes, we first tried to manually replace those spikes with linear interpolations. If the artifact identification was still problematic after manual denoising, the dataset was discarded.

The LFP data can be divided into several segments using the triggers, and there should be 1020 segments that contains gradient-induced artifacts in each scan. Those segments were averaged to obtain the noise template, which was then subtracted from the individual segments of the raw LFP signal to get the denoised LFP signal. This method takes care of the gradient artifacts in the second phase (25 ms after the trigger), but the residual artifacts in the first phase (0~25 ms after the trigger) were still overwhelming after subtracting the noise template, so the first 25 ms of the LFP data were replaced with linear interpolation.

The denoised LFP signal was then low-pass filtered to 100 Hz using to remove any residual artifacts, and downsampled from 12KHz to 500Hz to reduce file size and computation cost. These downsampled LFP signals were then used to calculate the band- limited power (BLP) in different frequency ranges (Delta 1~4Hz, Theta 4~8Hz, Alpha 8~12Hz, Beta Low 12~25Hz, Beta High 25~40Hz, Gamma 40~100Hz) using sliding window. The sliding window has a length of 1 second and 50% overlap (so the window moves 0.5 second every time to match the temporal resolution of fMRI data, which is 0.5 second as well) and is centered at the echo time of the fMRI scan for each TR index. Within each window, the power spectral density (PSD) function was calculated using Welch's method (4 segments, 50% overlap) and was integrated over different frequency bands to obtain the BLP time courses at the corresponding TR index. The BLP time courses were then band-pass filtered (0.01–0.1Hz for ISO and 0.01–0.25Hz for DMED (Pan et al., 2013)). After the pre-processing, the raw LFP data with a sampling rate of 12 KHz was converted to BLP time courses with a temporal resolution of 0.5 seconds and a duration of 1000 TRs, which is 8 min 20 sec long. For further BOLD triggered average analysis, the BLP time courses in every frequency band from the same scan was normalized by a common scaling factor such

that the standard deviation of the broadband power is equal to 1, which makes the datasets with various amplitudes comparable with each other.

5.4. FMRI Data Pre-processing

The fMRI data was preprocessed in the following procedure. A brain mask for each scan was obtained from the first image of the scan using active contour methods and was dilated by 2 voxels before running motion correction on SPM 12. The motion corrected image series were then spatially smoothed using a Gaussian kernel with a FWHM of 2.8 voxel (2.8*0.3mm = 0.84mm). Then global signal and linear drift regression, as well as band-pass filtering (0.01–0.1Hz for ISO and 0.01–0.25Hz for DMED) were performed voxel-wise. As a quality assurance step, the cross-correlation map of LFP bandlimited-power versus BOLD is calculated at the lag when the correlation is expected to reach the maximum (4 seconds for ISO and 2.5 seconds for DMED). If there are high LFP broadband power versus BOLD S1-seed cross-correlation, and a bilateral symmetry in BOLD S1- seeded correlation map, the dataset was considered as high-quality data and was proceeded to the next step. By these criteria, 22 scans under DMED from 10 rats and 32 scans under various ISO concentrations from 12 rats were selected out of 337 scans from 36 rats. The selected datasets were then normalized voxel-wise to produce the BOLD image series for the co-activation patterns analysis. For BOLD triggered average analysis, a ROI was manually selected based on the cross-correlation map, and the BOLD signal was averaged over the ROI. Finally, the BOLD signal averaged over the ROI was z-scored so that the averaged BOLD signal is comparable with other fMRI scans.

5.5. Co-deactivation Patterns (CDAPs)

In addition to co-activation patterns, we also calculated co- deactivation patterns (CDAPs). The CDAPs were calculated using the method described in (Liu et al., 2013). The CDAPs were obtained by applying thresholds to the LFP broadband power time course, similar to calculating CAPs except the BOLD frames were selected when LFP broadband power was lower than the threshold, and the sign of the averaged intensity was flipped for better comparison with the correlation map. The comparison between CAPs and CDAPs are shown in Figure S.6 and Figure S.7. Although the CAPs described in the original paper lost similarities when the thresholds are too low (because the co-deactivation frames cancel out the effect of the co-activation frames), however, we found that those co-deactivation frames do not always destroy the patterns, and solely using them can produce a nearly identical spatial map, which is in agreement with the findings in (Liu et al., 2013), though they generally requires more frames to achieve the same level of similarities. So the fact that CAPs can reproduce correlation map should be interpreted as co-activation frames contain information that is sufficient, but not necessary to resemble the correlation map. The underlying reason might be the complicated coupling in the timing of CAPs and CDAPs, which is probably induced by the nature of temporal filtering with a relatively narrow frequency band of the power time course.

Another thing to notice is that, the amount of frames needed to reach the similarity plateau is different for different CAPs. Generally speaking, BOLD-CAPs and BOLD-CDAPs are the two fastest to reach the plateau (need 5~10% of the data), followed by LFP-CAPs (need

around 20%), and the LFP-CDAPs is the slowest (may need up to 30%). It is implied that since the spatial patterns in the correlation map can be accurately replicated by only a small portion of dataset, those selected frames contains all the information needed for resembling the pattern. So it is reasonable to assume that, if fewer frames is needed for resembling the pattern, then each frame contains more information than otherwise. Since LFP is linked to BOLD signal through intermediate steps including hemodynamic functions, whereas BOLD signal is more directly tied to the BOLD signals in other region through the same mechanism, it is not surprising to see that BOLD-CAPs reach plateau quicker than LFP-CAPs. The fact that LFP-CAPs need fewer frames than LFP-CDAPs implies that the LFP activation is more dominant than deactivation when driving the LFP-BOLD relationship.

Supplementary Material

Refer to Web version on PubMed Central for supplementary material.

Acknowledgements

Funding sources: NIH 1 R01NS078095-01, BRAIN initiative and NSF INSPIRE. The authors would like to thank Chinese Scholarship Council (CSC) for financial support.

References

1. Ogawa S, Tank DW, Menon R, Ellermann JM, Kim SG, Merkle H, Ugurbil K. Intrinsic signal changes accompanying sensory stimulation: functional brain mapping with magnetic resonance imaging. Proceedings of the National Academy of Sciences. 1992 7 1;89(13):5951–5.
2. Biswal B, Zerrin Yetkin F, Haughton VM, Hyde JS. Functional connectivity in the motor cortex of resting human brain using echo - planar MRI. Magnetic resonance in medicine. 1995 10;34(4):537–41. [PubMed: 8524021]
3. Fox MD, Raichle ME. Spontaneous fluctuations in brain activity observed with functional magnetic resonance imaging. Nature reviews neuroscience. 2007 9;8(9):700. [PubMed: 17704812]
4. Cordes D, Haughton VM, Arfanakis K, Wendt GJ, Turski PA, Moritz CH, Quigley MA, Meyerand ME. Mapping functionally related regions of brain with functional connectivity MR imaging. American Journal of Neuroradiology. 2000 10 1;21(9):1636–44. [PubMed: 11039342]
5. Hampson M, Peterson BS, Skudlarski P, Gatenby JC, Gore JC. Detection of functional connectivity using temporal correlations in MR images. Human brain mapping. 2002 4;15(4):247–62. [PubMed: 11835612]
6. Greicius MD, Krasnow B, Reiss AL, Menon V. Functional connectivity in the resting brain: a network analysis of the default mode hypothesis. Proceedings of the National Academy of Sciences. 2003 1 7;100(1):253–8.
7. Fox MD, Corbetta M, Snyder AZ, Vincent JL, Raichle ME. Spontaneous neuronal activity distinguishes human dorsal and ventral attention systems. Proceedings of the National Academy of Sciences. 2006 6 27;103(26):10046–51.
8. Smith SM, Fox PT, Miller KL, Glahn DC, Fox PM, Mackay CE, Filippini N, Watkins KE, Toro R, Laird AR, Beckmann CF. Correspondence of the brain's functional architecture during activation and rest. Proceedings of the National Academy of Sciences. 2009 8 4;106(31):13040–5.
9. Keilholz SD. The neural basis of time-varying resting-state functional connectivity. Brain connectivity. 2014 12 1;4(10):769–79. [PubMed: 24975024]
10. Thompson GJ. Neural and metabolic basis of dynamic resting state fMRI. Neuroimage. 2018 10 15;180:448–62. [PubMed: 28899744]
11. Logothetis NK, Pauls J, Augath M, Trinath T, Oeltermann A. Neurophysiological investigation of the basis of the fMRI signal. Nature. 2001 7;412(6843):150. [PubMed: 11449264]

12. Gaudes CC, Petridou N, Dryden IL, Bai L, Francis ST, Gowland PA. Detection and characterization of single - trial fMRI bold responses: Paradigm free mapping. Human brain mapping. 2011 9 1;32(9):1400–18. [PubMed: 20963818]

13. Gaudes CC, Petridou N, Francis ST, Dryden IL, Gowland PA. Paradigm free mapping with sparse regression automatically detects single-trial functional magnetic resonance imaging blood oxygenation level dependent responses. Human brain mapping. 2013 3 1;34(3):501–18. [PubMed: 22121048]

14. Petridou N, Gaudes CC, Dryden IL, Francis ST, Gowland PA. Periods of rest in fMRI contain individual spontaneous events which are related to slowly fluctuating spontaneous activity. Human brain mapping. 2013 6;34(6):1319–29. [PubMed: 22331588]

15. Tagliazucchi E, Balenzuela P, Fraiman D, Montoya P, Chialvo DR. Spontaneous BOLD event triggered averages for estimating functional connectivity at resting state. Neuroscience letters. 2011 1 20;488(2):158–63. [PubMed: 21078369]

16. Tagliazucchi E, Balenzuela P, Fraiman D, Chialvo DR. Criticality in large-scale brain fMRI dynamics unveiled by a novel point process analysis. Frontiers in physiology. 2012a 2 8;3:15. [PubMed: 22347863]

17. Liu X, Duyn JH. Time-varying functional network information extracted from brief instances of spontaneous brain activity. Proceedings of the National Academy of Sciences. 2013 3 12;110(11):4392–7.

18. Liu X, Chang C, Duyn JH. Decomposition of spontaneous brain activity into distinct fMRI co-activation patterns. Frontiers in systems neuroscience. 2013 12 4;7:101. [PubMed: 24550788]

19. Wu GR, Liao W, Stramaglia S, Ding JR, Chen H, Marinazzo D. A blind deconvolution approach to recover effective connectivity brain networks from resting state fMRI data. Medical image analysis. 2013 4 1;17(3):365–74. [PubMed: 23422254]

20. Amico E, Gomez F, Di Perri C, Vanhaudenhuyse A, Lesenfants D, Boveroux P, Bonhomme V, Brichant JF, Marinazzo D, Laureys S. Posterior cingulate cortex-related co- activation patterns: a resting state fMRI study in propofol- induced loss of consciousness. PLoS One. 2014 6 30;9(6):e100012. [PubMed: 24979748]

21. Li W, Li Y, Hu C, Chen X, Dai H. Point process analysis in brain networks of patients with diabetes. Neurocomputing. 2014 12 5;145:182–9.

22. Allan TW, Francis ST, Caballero-Gaudes C, Morris PG, Liddle EB, Liddle PF, Brookes MJ, Gowland PA. Functional connectivity in MRI is driven by spontaneous BOLD events. PloS one. 2015 4 29;10(4):e0124577. [PubMed: 25922945]

23. Chen JE, Chang C, Greicius MD, Glover GH. Introducing co- activation pattern metrics to quantify spontaneous brain network dynamics. Neuroimage. 2015 5 1;111:476–88. [PubMed: 25662866]

24. Tagliazucchi E, Siniatchkin M, Laufs H, Chialvo DR. The voxel-wise functional connectome can be efficiently derived from co-activations in a sparse spatio-temporal point-process. Frontiers in neuroscience. 2016 8 23;10:381. [PubMed: 27601975]

25. Liu X, De Zwart JA, Schölvinck ML, Chang C, Frank QY, Leopold DA, Duyn JH. Subcortical evidence for a contribution of arousal to fMRI studies of brain activity. Nature communications. 2018a 1 26;9(1):395.

26. Turchi J, Chang C, Frank QY, Russ BE, David KY, Cortes CR, Monosov IE, Duyn JH, Leopold DA. The basal forebrain regulates global resting-state fMRI fluctuations. Neuron. 2018 2 21;97(4):940–52. [PubMed: 29398365]

27. Liang Z, Liu X, Zhang N. Dynamic resting state functional connectivity in awake and anesthetized rodents. Neuroimage. 2015 1 1;104:89–99. [PubMed: 25315787]

28. Shmuel A, Augath M, Oeltermann A, Logothetis NK. Negative functional MRI response correlates with decreases in neuronal activity in monkey visual area V1. Nature neuroscience. 2006 4;9(4):569. [PubMed: 16547508]

29. Huttunen JK, Gröhn O, Penttonen M. Coupling between simultaneously recorded BOLD response and neuronal activity in the rat somatosensory cortex. Neuroimage. 2008 1 15;39(2):775–85. [PubMed: 17964186]

30. Shmuel A, Leopold DA. Neuronal correlates of spontaneous fluctuations in fMRI signals in monkey visual cortex: implications for functional connectivity at rest. Human brain mapping. 2008 7;29(7):751–61. [PubMed: 18465799]

31. Murayama Y, Bieβmann F, Meinecke FC, Müller KR, Augath M, Oeltermann A, Logothetis NK. Relationship between neural and hemodynamic signals during spontaneous activity studied with temporal kernel CCA. Magnetic resonance imaging. 2010 10 1;28(8):1095–103. [PubMed: 20096530]

32. Pan WJ, Thompson G, Magnuson M, Majeed W, Jaeger D, Keilholz S. Broadband local field potentials correlate with spontaneous fluctuations in functional magnetic resonance imaging signals in the rat somatosensory cortex under isoflurane anesthesia. Brain connectivity. 2011 8 1;1(2):119–31. [PubMed: 22433008]

33. Mishra AM, Ellens DJ, Schridde U, Motelow JE, Purcaro MJ, DeSalvo MN, et al. Where fMRI and electrophysiology agree to disagree: corticothalamic and striatal activity patterns in the WAG/Rij rat. Journal of Neuroscience. 2011 10 19;31(42):15053–64. [PubMed: 22016539]

34. Magri C, Schridde U, Murayama Y, Panzeri S, Logothetis NK. The amplitude and timing of the BOLD signal reflects the relationship between local field potential power at different frequencies. Journal of Neuroscience. 2012 1 25;32(4):1395–407. [PubMed: 22279224]

35. Devonshire IM, Papadakis NG, Port M, Berwick J, Kennerley AJ, Mayhew JE, Overton PG. Neurovascular coupling is brain region-dependent. Neuroimage. 2012 2 1;59(3):1997–2006. [PubMed: 21982928]

36. Pan WJ, Thompson GJ, Magnuson ME, Jaeger D, Keilholz S. Infraslow LFP correlates to resting-state fMRI BOLD signals. Neuroimage. 2013 7 1;74:288–97. [PubMed: 23481462]

37. Tagliazucchi E, Von Wegner F, Morzelewski A, Brodbeck V, Laufs H. Dynamic BOLD functional connectivity in humans and its electrophysiological correlates. Frontiers in human neuroscience. 2012b 12 28;6:339. [PubMed: 23293596]

38. Dayan P, Abbott LF. Theoretical neuroscience: computational and mathematical modeling of neural systems. MIT Press, Cambridge, MA, pp 17–23.

39. Liu X, Zhang N, Chang C, Duyn JH. Co-activation patterns in resting-state fMRI signals. Neuroimage. 2018b 10 15;180:485–94. [PubMed: 29355767]

40. Power JD, Barnes KA, Snyder AZ, Schlaggar BL, Petersen SE. Spurious but systematic correlations in functional connectivity MRI networks arise from subject motion. Neuroimage. 2012 2 1;59(3):2142–54. [PubMed: 22019881]

41. Magnuson ME, Thompson GJ, Pan WJ, Keilholz SD. Time- dependent effects of isoflurane and dexmedetomidine on functional connectivity, spectral characteristics, and spatial distribution of spontaneous BOLD fluctuations. NMR in biomedicine. 2014 3;27(3):291–303. [PubMed: 24449532]

42. Liu X, Zhu XH, Zhang Y, Chen W. Neural origin of spontaneous hemodynamic fluctuations in rats under burst–suppression anesthesia condition. Cerebral cortex. 2010 6 7;21(2):374–84. [PubMed: 20530220]

43. Pan WJ, Thompson G, Magnuson M, Majeed W, Jaeger D, Keilholz S. Simultaneous FMRI and electrophysiology in the rodent brain. Journal of Visualized Experiments. 2010 8 19(42):e1901.

44. Automatic Gruetter R., localized in vivo adjustment of all first- and second-order shim coils. Magnetic resonance in medicine. 1993 6;29(6):804–11. [PubMed: 8350724]

45. Pawela CP, Biswal BB, Hudetz AG, Schulte ML, Li R, Jones SR, Cho YR, Matloub HS, Hyde JS. A protocol for use of medetomidine anesthesia in rats for extended studies using task-induced BOLD contrast and resting-state functional connectivity. Neuroimage. 2009 7 15;46(4):1137–47. [PubMed: 19285560]

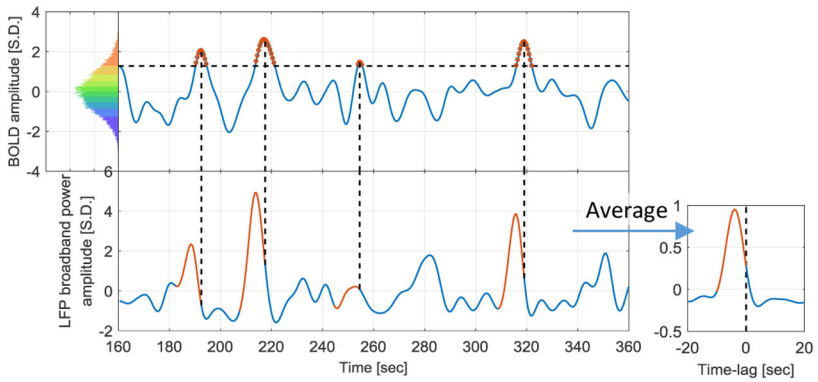

Figure 1. Illustration of the procedure to obtain the BOLD-triggered average time course.

The data shown is from the ISO group (32 scans, each containing 1000 time points). The pooled distribution is evenly divided into 10 groups, each containing 3200 samples (red for high BOLD value and blue for low BOLD value, this color-coding applies to all figures that involve BOLD amplitude groups). A 200-second segment of a particular scan is plotted to illustrate the procedure. For a selected BOLD group (90~100% BOLD is shown), the thresholds were obtained from the pooled distribution (>1.28 BOLD S.D. for this group), and applied to the time course to identify those time points as the BOLD events (marked in red circles on the top). Then the corresponding LFP segments proceeding the BOLD events were extracted (red segments on the bottom) and averaged across all 32 scans to obtain the BOLD-triggered average time course. For display purposes, only four LFP segments were shown.

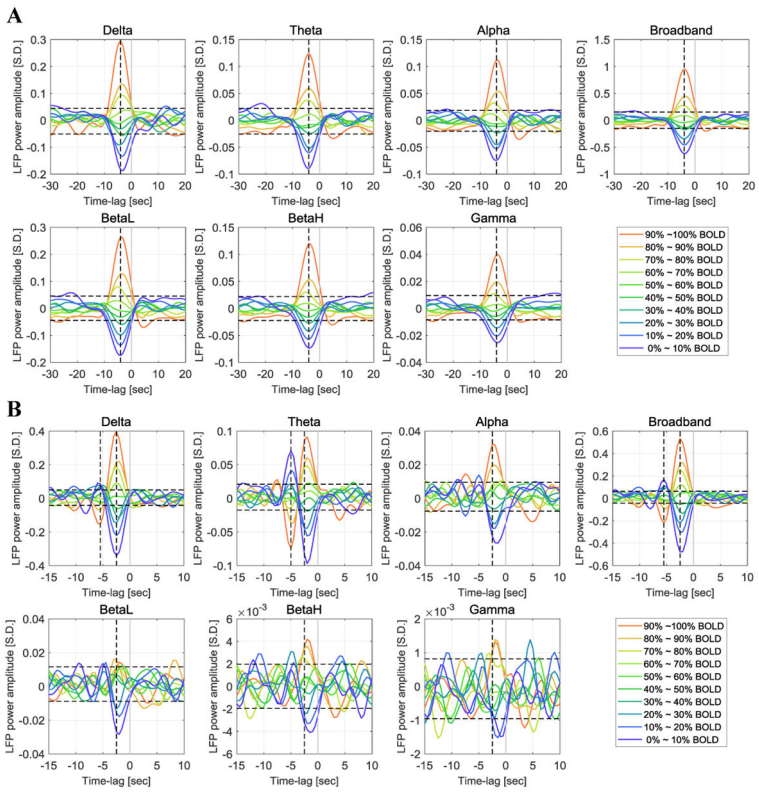

Figure 2. Time courses of the BOLD-triggered average of LFP power in different frequency bands under ISO anesthesia (panel A, 32 scans) and DMED anesthesia (panel B, 22 scans).

The x-axis is the time lag with respect to the BOLD triggers. The y-axis is the normalized LFP power (the standard deviation of broadband LFP power is 1 LFP S.D.). The vertical cursors show the maximally-correlated lag (−4 seconds for ISO in all frequency bands; −2.5 second for DMED in all frequency bands, with an additional line for the negative deviation which is located at −5.5 seconds for Delta band and Broadband, and at −5 seconds for Theta band). Each point in the time courses is the averaged value of roughly 10% of the dataset. The upper threshold and lower threshold for 95% confidence intervals are obtained from the 97.5 and 2.5 percentiles of the noise empirical distribution, respectively. BetaL, low frequency beta 12~25Hz, BetaH, high frequency beta, 25~40Hz.

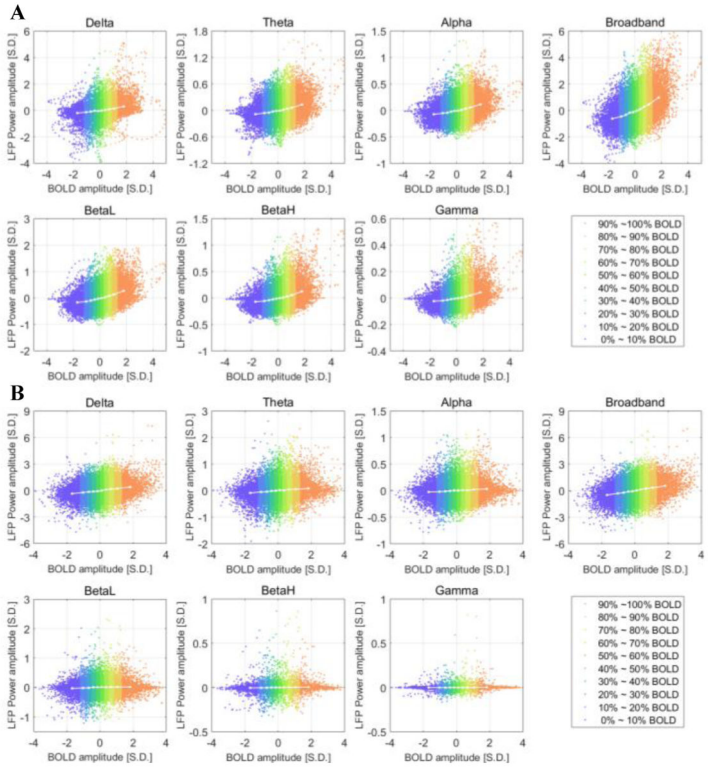

Figure 3. Scatter plot of LFP vs BOLD and the centroids of each BOLD group under ISO (panel A, 32 scans) and DMED (panel B, 22 scans).

Each dot represents a time point with its BOLD value and LFP power value. Since each scan session has 1000 time points, each plot in panel A consists of 32000 points, and each plot in panel B consists of 22000 points. The time delay is already adjusted (the LFP power is delayed by 4 seconds under ISO and 2.5 seconds under DMED). Each centroid shows the averaged LFP power within each BOLD group. The centroids are essentially showing the BOLD-triggered averages at the maximally-correlated lag, which are the value specified by the vertical cursors in Figure 2.

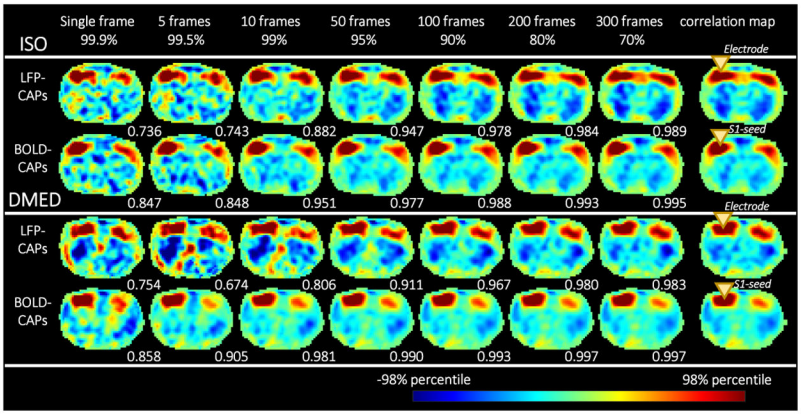

Figure 4. Co-activation patterns become more similar to the correlation map as more frames are included for calculation.

From left to right, as the threshold (shown in percentiles) become lower, more frames are included. The LFP-BOLD correlation map (at the maximally correlated lag) and BOLD S1-seeded correlation map are shown on the far right (the yellow triangles show the location of the electrode and the S1-seed). For each CAP, the spatial similarity with regard to the correlation map is shown in the bottom right corner of each image. It can be seen that the spatial similarity increases very quickly as more frames are included, and reaches a plateau near 1 when a certain amount of frames are included. Even if only 10%~20% of the dataset is used, most CAPs can replicate a spatial pattern nearly identical to the correlation map, which is calculated from the entire dataset. Each image is normalized by its 98 percentile to enable easier comparison of the spatial patterns.

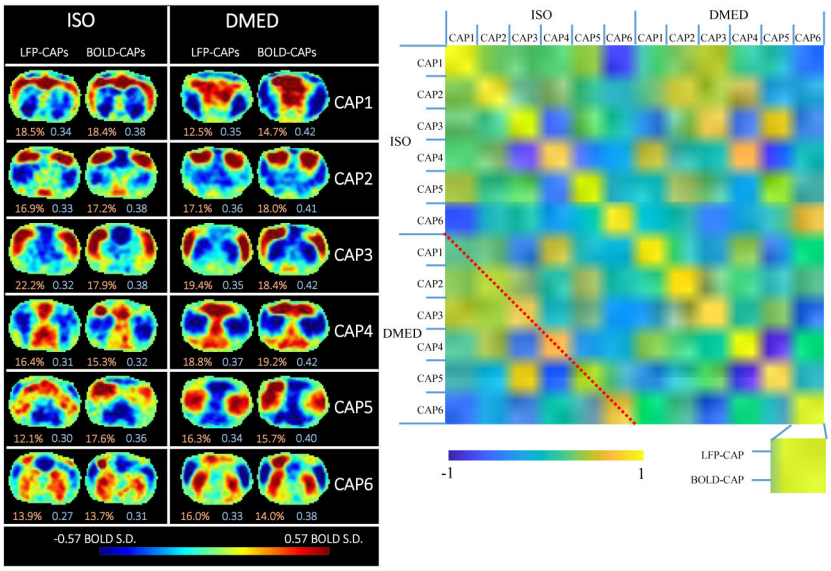

Figure 5. Temporal decomposition of the selected co-activation frames (left) and the similarity matrix (right).

The frames selected based on high amplitude events are further divided into six clusters using the k-means algorithm (k=6) to produce CAPs. The threshold used for selecting frames was 15% for both LFP-CAPs and BOLD-CAPs. The LFP-CAPs under ISO are sorted based on the consistency (the average spatial similarity of each fMRI frame to the group mean). The LFP-CAPs under DMED are sorted to maximize the summed spatial similarity between LFP-CAPs under ISO and LFP-CAPs under DMED (for easier comparison across different anesthetic conditions). The BOLD-CAPs are also sorted in a similar way using LFP-CAPs as the benchmark. The consistency (light red) and fraction values (light blue) of the CAPs are shown on the bottom of each image. The similarity matrix shows the spatial similarity (Pearson correlation) between any combinations of two CAPs. Within each anesthetic agent group, there are 6 different CAPs groups. Within each CAP group, there are also two elements: LFP-CAP and BOLD-CAP, giving 24x24 elements visualized in this matrix

Table 1.

Guidelines of data quality metrics

	Good	Fair	Poor
LFP			
Number of gradient induced artifact	=1020		≠1020
Residual noise in LFP	No large spike in de-noised LFP		More tdan one large spike in de-noised LFP
BOLD			
Trajectory of center of mass	abs(Δx) ≤ 0.05 pixel and abs(Δy) ≤ 0.05 pixel	abs(Δx) ≤ 0.1 pixel and abs(Δy) ≤ 0.1 pixel and either abs(Δx) ≥ 0.05 pixel or abs(Δy) ≥ 0.05 pixel	abs(Δx) ≥ 0.1 pixel or abs(Δy) ≥ 0.1 pixel
DVARS	DVARS ≤ 0.5%	0.5% ≤ DVARS ≤ 1% and the number of small spikes is fewer than 5	Either DVARS ≥ 1% (large spikes) or the number of small spikes is more than 5
Image distortion	No noticeable image distortion or signal loss		Noticeable image distortion or signal loss
Function connectivity (correlation between bilateral S1 areas)	Correlation ≥ 0.3 and the correlation map is localized to somatosensory network	Correlation ≥ 0.15 and either correlation ≤ 0.3 or the correlation map is not completely localized	Correlation ≤ 0.15 or unlocalized correlation
LFP-BOLD correlation	Correlation ≥ 0.2 for both S1 areas and the correlation map is well-localized to sites surrounding electrodes	Correlation ≥ 0.1 and either correlation ≤ 0.2 or the correlation map is not completely localized	Correlation ≤ 0.1 or unlocalized correlation